

Fast thermal escape of carbon and oxygen from a dense, CO₂-rich early martian atmosphere

Feng Tian^{1,2}, James F. Kasting³, Stanley C. Solomon²

1. NASA Postdoctoral Program at NASA Astrobiology Institute

2. High Altitude Observatory, National Center for Atmospheric Research, 3080 Center Green, Boulder, CO 80301

3. Department of Geosciences, Penn State University, University Park, PA 16802

Abstract:

Self-consistent hydrodynamic models of Mars' thermosphere suggest that both carbon and oxygen could have escaped thermally from the planet during its early history, when the solar extreme ultraviolet (EUV) flux was high. Such thermal escape could have been much faster than nonthermal escape mechanisms considered by other investigators. This rapid loss of C and O implies that CO₂ could not have accumulated to high concentrations in Mars' earliest atmosphere, suggesting that Mars began its life cold. By 3.9 billion years (b.y.) ago, the solar EUV flux should have declined substantially, and the thermal escape timescale of carbon would have become long enough to allow a dense CO₂ atmosphere to accumulate, provided that sufficient CO₂ was still being outgassed. An ensuing warm, wet period lasting of the order of a few hundred million years could then have allowed fluvial features to form. Thermal escape of carbon and oxygen would have become negligible by 3.5 b.y. ago, but nonthermal escape mechanisms could have subsequently removed 1-2 bar of additional CO₂, leaving little of it behind on Mars' surface.

Geomorphological and geochemical features suggest that Mars was wet and relatively warm during the latter part of the Noachian period, which ended ~3.7 b.y. ago (1,2,3). The early Noachian, prior to 4.3 b.y. ago, shows less evidence for fluvial modification—a signal that could be caused either by a colder climate or simply by lack of preservation (4). Roughly 1-5 bars of CO₂ are thought to have been needed in order to raise the global mean surface temperature of early Mars above the freezing point of water (5,6), although no one has demonstrated that this mechanism actually works for plausible assumptions about CO₂ cloud cover (7), and hence other, colder scenarios for valley formation have been proposed (8). To account for the present tenuous martian atmosphere, this postulated dense early CO₂ atmosphere must have been lost either to the surface or to space. Significant carbonate outcrops have yet to be discovered on Mars (9), perhaps because surface conditions were highly acidic (10,11). This suggests that most of the dense CO₂ early Martian atmosphere may have been lost to space. To accomplish this, a variety of nonthermal loss mechanisms (12) have been proposed, including dissociative recombination (13,14), solar wind pickup (14), sputtering (15,16,17), and impact erosion (18). Thermal escape (19) for species heavier than He has in general been neglected.

Recent work (17,20) suggests that the oxygen loss rate by nonthermal escape processes from Mars at 3.5 b.y. ago should have been $\sim 2.5 \times 10^9 \text{ cm}^{-2} \text{ s}^{-1}$, or $2.5 \times 10^{27} \text{ s}^{-1}$ globally, somewhat slower than predicted by earlier calculations (14,15,16). At this rate, 120 mbar of oxygen could have been lost since that time. Nonthermal removal of carbon is more difficult: <100 mbar of CO₂ could have been lost by sputtering (17) in ~3.5 b.y. All of the above-mentioned nonthermal escape calculations are based on a thermosphere model in (14), in which the lower atmosphere was assumed to be the same as that of present Mars. The CO₂ number density at 150 km altitude in this model was $(2-4) \times 10^9 \text{ cm}^{-3}$. When EUV fluxes of 3x and 6x present were applied to this “thin” Mars atmosphere, the exobase altitude was found to be 216 km and 310 km, respectively, while the associated exobase temperatures were ~300 K and ~550 K (14). In this model, thermal escape was negligible compared with nonthermal escape processes. However, a dense CO₂ early martian atmosphere should have had a significantly denser thermosphere. The CO₂ number density at 150 km altitude in an atmosphere with a 2-bar surface pressure should be $> 3 \times 10^{11} \text{ cm}^{-3}$ (Supplemental Material), about 100 times greater than that assumed in (14).

We used a 1-D, multi-component, hydrodynamic, planetary thermosphere / ionosphere model (21) to investigate the upper atmosphere of a dense, CO₂-rich early Mars. An electron transport / energy deposition model was coupled to the thermosphere-ionosphere model to self-consistently calculate ionization/excitation rates of thermospheric constituents, along with the associated ambient electron heating rates (22). This approach allows us to avoid having to make arbitrary assumptions about EUV heating efficiencies. Some new physics and chemistry was added to the model for this study to make it applicable to CO₂-rich atmospheres. Electron impact cross sections for both CO₂ and CO were taken from (23). Transport and chemistry of atomic carbon was included in the model in order to investigate its escape. The model includes radiative cooling from the CO₂ 15- μm band (24), the NO 5.7- μm band (25), the O fine structure 63- μm band (26), and the CO 4.7- μm band (Supplemental Material). At the lower

boundary of the model (96 km altitude), fixed downward deposition velocities (Supplemental Material) were used for species such as C, O, and CO, which are formed in the thermosphere, and fixed mass mixing ratios were applied for other species (27).

Results from the model are shown in Figures 1-3. The solid curves in Fig. 1a represent the calculated neutral temperature profiles in four simulated martian atmospheres. The solid curves in Fig. 1b show the total number density profiles for the corresponding cases. The dashed curves are the density profiles of atomic oxygen, CO₂, and atomic carbon in Case 3. The calculated exobase temperature and altitude in Case 1 ($p_s=6$ mbar and 6x solar EUV) were 570 K and 550 km, respectively, similar to those in (14). Atomic oxygen was the dominant gas at the exobase in this case, and its escape parameter (29), λ_o , was 37, implying that it would not have escaped thermally. In Case 2, the exobase of this thin Martian atmosphere expanded under 10x present EUV flux to 1000 km altitude, and the exobase temperature rose to 1000 K. Consequently, λ_o dropped to 18, which is still too large to permit efficient thermal escape of O.

By contrast, a 2-bar CO₂ Martian atmosphere under the same solar EUV conditions (Case 3) would have been warmer and more expanded. Both atomic oxygen and carbon were abundant at the exobase. In Case 3, the exobase temperature and altitude were 2350 K and 6830 km (3 Mars radii), respectively. The escape parameters for C and O were $\lambda_c = 2.6$ and $\lambda_o = 3.4$, low enough to allow these species to readily escape. The weak gravity field of Mars was thus no match for the extreme solar EUV energy input from the early young Sun. In contrast, Earth and Venus, with their stronger gravity, remained well protected (30). When still stronger solar EUV fluxes were applied to the dense martian atmosphere (Case 4), the exobase moved further out to 17000 km altitude (6 Mars radii), and the temperature was 1950 K ($\lambda_c = 1.8$ and $\lambda_o = 2.3$). Atmospheric temperature decreased with altitude in the upper thermosphere because of cooling caused by adiabatic expansion, indicating that the martian thermosphere was in the hydrodynamic regime²¹.

Fig. 2 shows the calculated Jeans escape rates of atomic carbon and oxygen from a 2-bar CO₂ martian atmosphere under different solar EUV conditions. At 3.5 and 3.8 b.y. ago, the solar EUV fluxes were ~6x and 10x present, respectively (31). The calculated Jeans escape flux of carbon from a 2-bar CO₂ martian atmosphere is $7.5 \times 10^{10} \text{ cm}^{-2} \text{ s}^{-1}$ at 3.8 b.y. ago, and the time required to lose 2 bars of CO₂ is ~34 million years under this escape flux. Hence, such an atmosphere could only have been sustained if CO₂ were supplied by volcanic outgassing at this rate or faster (see below). The calculated Jeans escape rate of carbon decreased dramatically to $\sim 10^6 \text{ cm}^{-2} \text{ s}^{-1}$ at 3.5 b.y. ago as a consequence of the nonlinear response of the Martian thermosphere to reduced solar EUV flux. Based on the “thin” martian atmosphere model (14), ~60 mbar of CO₂ could have been lost through sputtering since 3.5 b.y. ago (17). Our calculations show that the CO₂ and CO densities in a 2-bar martian atmosphere should have been at least one order of magnitude greater than those in the ‘thin’ atmosphere model under the same level of solar EUV flux. Thus, it is likely that 1 or 2 bars of CO₂ could have been removed by nonthermal escape processes from Mars after thermal escape had become negligible.

Carbon would have escaped faster than oxygen from a dense CO₂ martian atmosphere under extreme solar EUV conditions (Fig. 2), simply because it is lighter. Because this carbon was derived originally from CO₂, the lower atmosphere of Mars should therefore have become enriched in O₂ on time scales comparable to that for CO₂ loss. O₂ should have accumulated in the lower atmosphere until escape of O to space was able to balance the escape of C, *i.e.*, until CO₂ itself was being lost. To model this more realistic situation, a series of simulations was performed with different lower boundary conditions on O₂. For the 10x present EUV condition (3.8 b.y. ago), steady state was achieved at an O₂ mass mixing ratio of 18% when the C escape rate ($4 \times 10^{10} \text{ cm}^{-2} \text{ s}^{-1}$) was half that of O. O density in this case is a factor of 3.5 greater than the C density at the exobase, located at 7800 km altitude. The exobase temperature in this case is 400 K warmer than that in the base (O₂-poor) case because the adiabatic cooling associated with the escape flow is the dominant cooling mechanism near the exobase and higher temperature is required for O to escape as efficiently as C does. Although we have not calculated this explicitly, the thermal escape of C and O should have fractionated their isotopes so that heavier isotopes were preferentially retained. Indeed, modest enrichments of heavy isotopes of C and O are observed in Mars' present atmosphere (2).

The evolutionary history of the early martian atmosphere can be inferred by comparing the calculated loss rates of C with estimated CO₂ volcanic outgassing rates, bearing in mind that the escape calculations assume a dense atmosphere. Fig. 3 shows the carbon loss rate from a 2-bar CO₂ atmosphere as a function of time (dashed curve). The solid lines represent a plausible range of CO₂ outgassing rates from early Mars (Supplemental Materials). The arrow marks the CO₂ outgassing rate from present Earth (32). Our lack of knowledge of the outgassing history of Mars prevents us from predicting exactly when the loss rate of carbon would have become smaller than the CO₂ volcanic outgassing rate. However, Fig. 3 indicates that the reduction of the solar EUV energy flux over time could have allowed a dense CO₂ atmosphere to have accumulated between 3.7 and 3.9 b.y. ago. It has been estimated that 1.5-3 bars of CO₂ were released volcanically during the late Noachian epoch during the formation of the Tharsis bulge (4). If all of this CO₂ was released into the atmosphere within 100 million years, the average CO₂ outgassing flux would have been comparable to the CO₂ escape flux ($\sim 2 \times 10^{10} \text{ cm}^{-2} \text{ s}^{-1}$) at 3.7 billion years ago (8x present EUV). A warm and wet early Mars could have been maintained for ~ 100 million years, during which widespread water erosion surface features could have formed. Nonthermal escape of carbon and oxygen from late Noachian Mars, combined with acidic conditions at the surface (10, 11), might explain the apparent absence of carbonate deposits.

These simulations neglect the H₂ that should also have been released from early martian volcanoes. On modern Earth, the ratio of H₂/CO₂ in volcanic gases is ~ 0.1 to 1 (33, 34). The H₂ released from volcanoes should have been largely balanced by loss to space (28); hence, H or H₂ should also have been escaping from early Mars, along with C and O. This should not have slowed the escape rate appreciably, however. Indeed, the presence of H and H₂ should have caused the martian thermosphere to be even more expanded, making it easier for all gases to escape. Our calculations also neglect nonthermal escape processes, which could have added to the escape flux of C and O.

However, such nonthermal escape processes are thought to have been inhibited during the early Noachian by the presence of a strong, dynamo-generated martian magnetic field (35, 3). By contrast, the thermal escape process modeled here affects neutral gases and should have been more or less independent of magnetic field strength.

Our results suggest that early Mars may have been cold and dry during the early Noachian, except perhaps during relatively short periods following large volcanic outgassing events. Volatiles, including H₂O and CO₂, would have been trapped on the surface of a cold early Mars and may thereby have been protected from escape to space. Later outgassing episodes, which occurred after the solar EUV flux had declined, may have warmed the climate sufficiently to release these trapped volatiles, thereby bolstering the atmospheric greenhouse. Such a scenario corresponds well with observed features on Mars' surface.

It has been hypothesized that conditions on early Mars were basically similar to those on Earth during the first several hundred million years of the planets' histories, in the sense that the environments on both planets were favorable to the existence of stable liquid water. The divergence between the two planets was considered to have occurred later as a consequence of fast nonthermal escape associated with solar wind interactions after the disappearance of Mars' intrinsic magnetic field. Our work suggests that Earth and Mars diverged at the very earliest stages of their evolutionary histories, and it highlights the importance of a planet's mass in retaining an atmosphere and maintaining habitability.

References and Notes

1. V.R. Baker, *Nature* 412, 228 (2001).
2. B. M. Jakosky, R. J. Phillips, *Nature* 412, 237 (2001).
3. S. C. Solomon *et al.*, *Science* 307, 1214 (2005).
4. R.J. Phillips *et al.*, *Science* 291, 2587 (2001).
5. J.F. Kasting, *Icarus* 94, 1 (1991).
6. F. Forget, R.T. Pierrehumbert, *Science* 278, 1273 (1997).
7. M.M. Mischna, J. F. Kasting, A. A. Pavlov, R. Freedman, *Icarus* 145, 546 (2000).
8. T. L. Segura, O. B. Toon, A. Colaprete, K. Zahnle, *Science* 298, 1977 (2002).
9. J.L. Bandfield, T.D. Glotch, P.R. Christensen, *Science* 307, 1576 (2003).
10. A.G. Fairen, D. Fernandez-Remolar, J.M. Dohn, V.R. Baker, R. Amils, *Nature* 431, 423 (2004).
11. I. Halevy, M.T. Zuber, D.P. Schrag, *Science* 318, 1903 (2007).
12. Nonthermal loss processes are those in which the escaping species has a mean velocity greater than that predicted by a Maxwellian velocity distribution at the ambient neutral temperature. Impact erosion, in which species of different molecular weights are removed indiscriminately, is an extreme form of nonthermal escape.
13. M.B. McElroy, *Science* 175, 443 (1972).
14. M.H.G. Zhang, J.G. Luhmann, S.W. Bougher, and A.F. Nagy, *JGR* 98, 10915 (1993).
15. J.G. Luhmann, R.E. Johnson, M.H.G. Zhang, *GRL* 19, 2151 (1992).

16. D.M. Kass and Y.L. Yung, *Science* 268, 697 (1995).
17. F. Leblanc, R.E. Johnson, J.G.R. 107, 5010, 10.1029/2000JE001473 (2002).
18. H.J. Melosh, A. M. Vickery, *Nature* 338, 487 (1989).
19. Thermal escape includes classical Jeans escape, in which the background atmosphere is hydrostatic and atoms in the high-energy tail of the Maxwellian velocity distribution evaporate into space from the exobase, along with full-blown, transonic hydrodynamic escape, in which the atmosphere remains collisional out to large distances so that the flow can be described by the equations of hydrodynamics. Except for the highest EUV cases, the solutions found here are intermediate between these two extremes: the flow is subsonic, an exobase can be defined at an altitude where the atmosphere becomes collisionless, and so Jeans escape boundary conditions can be applied at this distance.
20. H. Lammer, H.I.M. Lichtenegger, C. Kolb, I. Ribas, E.F. Guinan, R. Abart, S.J. Bauer, *Icarus* 165, 9 (2003).
21. F. Tian, J.F. Kasting, H. Liu, R.G. Roble, *JGR-planet*, in press <http://start.org/contents/journals/ViewPapersinPress.do?journalCode=JE> (2008a).
22. F. Tian, S.C. Solomon, L. Qian, J. Lei, R.G. Roble, *JGR-planets*, submitted (2008b).
23. T. Sawada, D.J. Strickland, A.E.S. Green, *JGR* 77, 4812 (1972).
24. B.F. Gordiets, Y.N. Kulikov, M.N. Markov, M.Y. Marov, *JGR* 87, 4504 (1982).
25. G. Kockarts, *GRL* 7, 137 (1980).
26. D.A. Glenar, E. Bleuler, J.S. Nisbet, *JGR* 83, 5550 (1978).
27. The mass mixing ratios assumed at the lower boundary for the 2-bar, CO₂-rich atmosphere were 99.999% for CO₂, 1.5x10⁻⁴ for N₂, 1.4x10⁻⁴ for O₂, and 5x10⁻¹¹ for H₂. The O₂ mixing ratio is approximately what is expected in the upper atmosphere of an abiotic early Earth (28), while the H₂ mixing ratio is several orders of magnitude lower than would be expected. Both of these would likely have been too low for early Mars, and so we will revisit these assumptions below.
28. J. F. Kasting, *Science* 259, 920 (1993).
29. The escape parameter $\lambda = \frac{GMm}{kTr}$ where G is the gravitational constant, M is the mass of the planet, m is the mass of escaping particle, k is the Boltzmann constant, and T and r are the temperature and radial distance at the exobase. The Jeans escape flux can be expressed as: $F_{Jeans} = \sqrt{\frac{kT}{2\pi m}} n(1 + \lambda)e^{-\lambda}$, where n is the number density of the escaping particles.
30. Comparative studies of the thermosphere of a CO₂-dominated early Venus under 10x present EUV flux at Venus' orbit give an exobase temperature and altitude of ~1900 K and ~700 km, respectively. The degree of thermosphere expansion and thermal escape from early Venus are significantly smaller than that of Mars because of its strong gravity. Escape from early Earth's atmosphere is even more difficult because of its slightly stronger gravity and greater orbital distance from the Sun. Thus, both Venus and Earth were better protected from loss of C and O than was Mars.
31. I. Ribas, E.F. Guinan, M. Gudel, M. Audard, *ApJ* 622, 680 (2005).
32. N. H. Sleep, K. Zahnle, *J. Geophys. Res.* 106, 1373 (2001).
33. H. D. Holland, *Geochim. Cosmochim. Acta* 66, 3811 (2002).
34. D. Canfield, M. T. Rosing, C. Bjerrum, *Phil. Trans. Roy. Soc. B* 361, 1819 (2006).
35. R. Lundin, *Science* 291, 1909 (2001)

36. F. T. is supported by the NASA Postdoctoral Program through the NASA Astrobiology Institute under Cooperative Agreement No. CAN-00-OSS-01. J.F.K acknowledges support from NASA Exobiology grant #NNG05G088G. S.C.S acknowledges support from NASA grant NNX07AC55G to the National Center for Atmospheric Research. The National Center for Atmospheric Research is supported by the National Science Foundation.

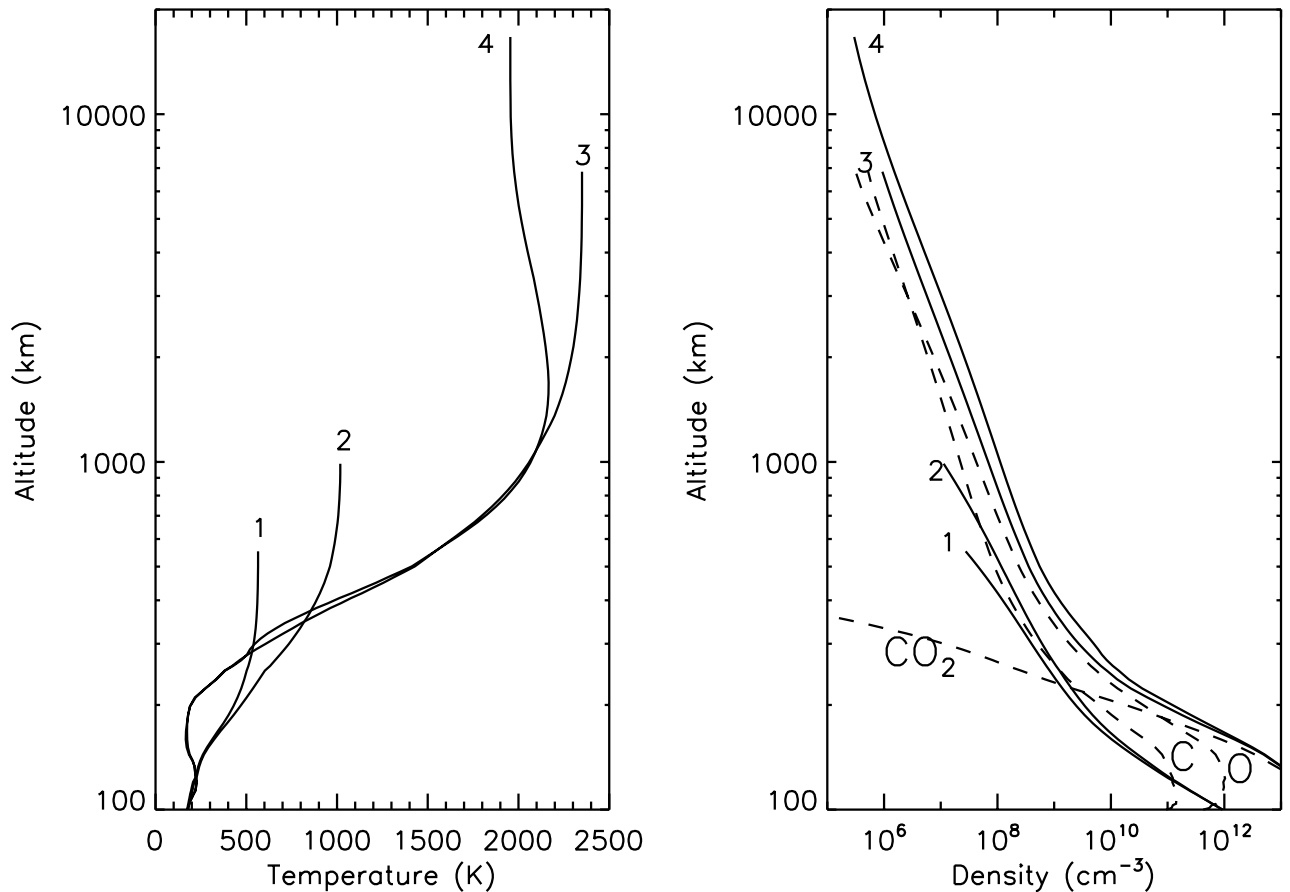


Fig. 1a: The solid curves are the calculated neutral temperature profiles in different martian atmospheres (Case 1: surface pressure $p_s=6$ mbar and 6x present solar EUV; Case 2: $p_s=6$ mbar and 10x present solar EUV; Case 3: $p_s=2$ bars and 10x present solar EUV; Case 4: $p_s=2$ bars and 17x present solar EUV). Fig. 1b: The solid curves are the total number density profiles for corresponding cases in panel a. The dashed curves are the density profiles of CO_2 , atomic oxygen, and atomic carbon in case 3.

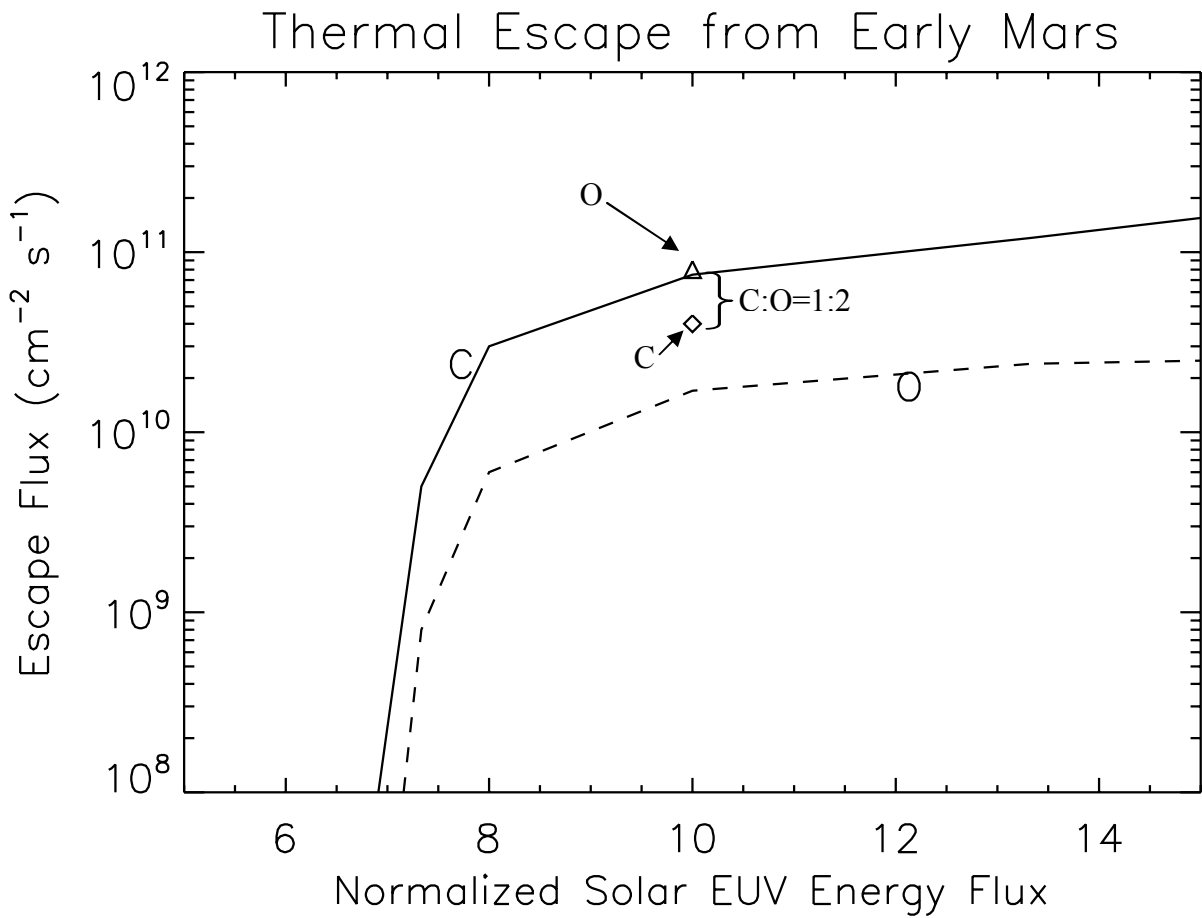


Fig. 2: The solid curve represents the Jeans escape rate of atomic carbon from a 2-bar CO₂ Martian atmosphere under different solar EUV conditions (normalized to the solar EUV energy flux under present solar mean condition). The dashed curve represents Jeans escape of atomic oxygen from the corresponding cases. The diamond and the triangle represent the Jeans escape rate of carbon and oxygen from a steady-state 2-bar Martian atmosphere (containing 18% O₂ and 82% CO₂), in which the oxygen escape rate is exactly twice that of carbon.

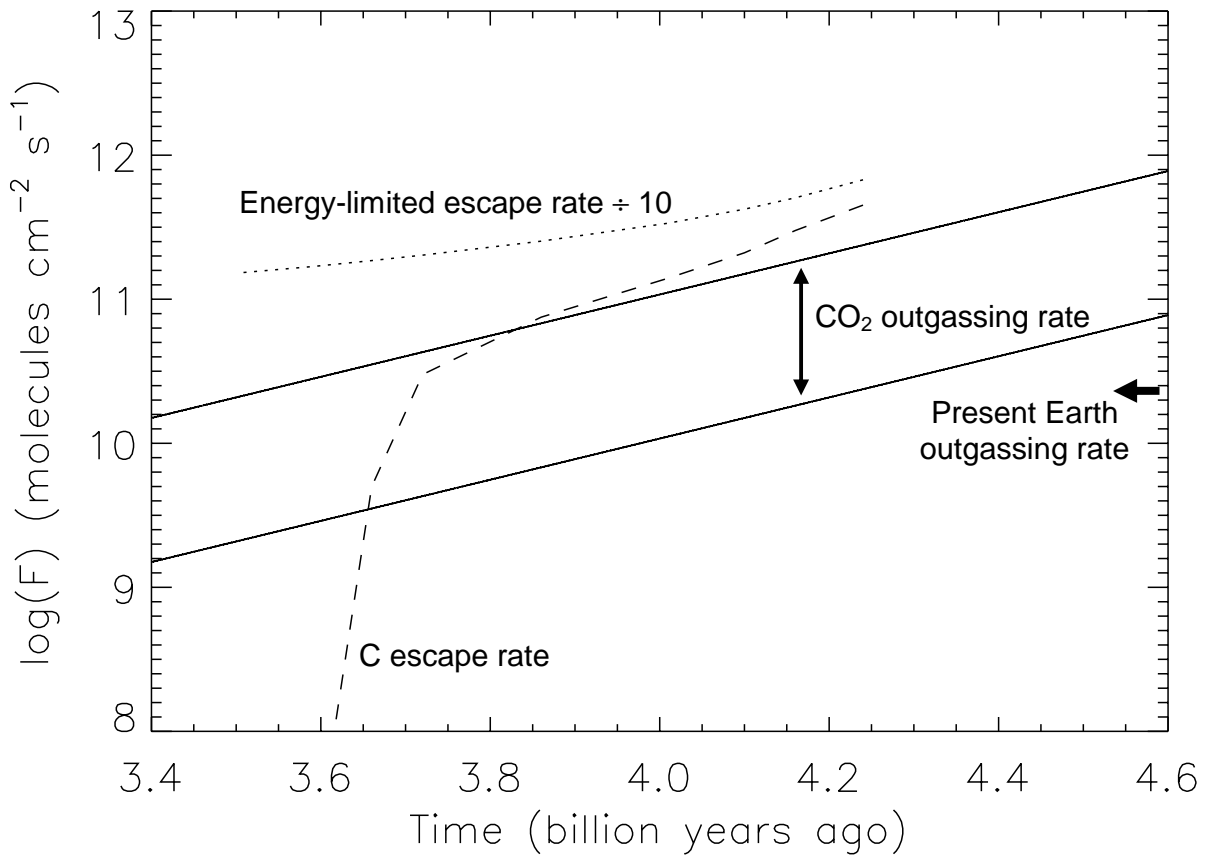


Fig. 3: The dashed curve represents the Jeans escape flux of atomic carbon from a 2-bar CO₂ atmosphere. The dotted curve represents 10% of the energy-limited escape flux of carbon from the corresponding atmosphere (Supplemental Material). The 2 solid lines represent possible CO₂ volcanic outgassing fluxes on early Mars. The small arrow marks the present Earth CO₂ outgassing flux (6×10^{12} moles per year, or $2.3 \times 10^{10} \text{ cm}^{-2} \text{ s}^{-1}$).

Supplemental materials:

Number density at 96 km and 150 km altitudes for a 2-bar CO₂ Martian atmosphere:

Assuming that the surface temperature is 273 K, the surface number density of a 2-bar CO₂ martian atmosphere is $5.3 \times 10^{19} \text{ cm}^{-3}$. The stratospheric temperature in a warm early Martian atmosphere is $\sim 150 \text{ K}$. The scale height in the troposphere is $\sim 10.6 \text{ km}$, using an average temperature of 210 K. Thus, the tropopause number density is $\sim 7.2 \times 10^{18} \text{ cm}^{-3}$ (at $\sim 21 \text{ km}$ altitude). The scale height in the stratosphere is $\sim 7.7 \text{ km}$, using a constant 150 K temperature. Using a constant scaleheight 7.7 km between 21 km and 150 km, the number density at 96 km and 150 km altitudes for a 2-bar CO₂ martian atmosphere should be $4.1 \times 10^{14} \text{ cm}^{-3}$ and $3.6 \times 10^{11} \text{ cm}^{-3}$, respectively. Considering the higher temperature in the lower thermosphere and the reduction of gravity with altitude, the actual number density at 150 km altitude should be even greater.

Downward deposition velocities of O and CO:

O and CO are formed through photodissociation of CO₂ and are transported downward to the lower atmosphere, where they should recombine to form CO₂. This process occurs on present Venus and explains the deficiency of O₂ and the dominance of CO₂ on that planet (von Zahn et al. 1983). The downward deposition velocities of O and CO are $\sim 100 \text{ cm/s}$ in the case of present Venus due to high eddy diffusion. Similar values are used in our model for the early dense CO₂ atmosphere of Mars. The density distributions of O and CO in the lowest 100 km are affected by the deposition velocities settings. However, because CO₂ is the dominant gas in the lower thermosphere, the model results are insensitive to the assumed deposition velocities.

CO 4.7- μm band cooling:

The CO 4.7- μm band cooling is treated similarly to the NO 5.7- μm band cooling (Kockarts 1980). The expressions in Chin and Weaver (1984) are used to compute Einstein A-coefficients. For simplicity, an average value of 16.3 s^{-1} is used for all ro-vibrational transitions between $v=1$ and $v=0$ states.

For collisional excitation and de-excitation coefficients, the expression given in Lopez-Puertas et al. (1993) is only valid over a limited temperature range. Thus, we use the theoretical expression in Chin and Weaver (1984): $k_{10} = \sigma v$ where σ is the cross section for CO to experience a rotation-vibration transition, which is weakly dependent on temperature, and v is the average relative speed between CO and its impactors. By comparing the rate coefficient computed using Chin-Weaver expression with that from Lopez-Puertas et al. (1993), we find that the rate coefficient should be in the order of $10^{-10} \text{ cm}^3 \text{ s}^{-1}$. In calculations we use $5 \times 10^{-11} \text{ cm}^3 \text{ s}^{-1}$, which is comparable to that of NO (Kockarts 1980).

Variation of Solar EUV Flux with Time:

Fig. S1 is produced with the analytical expression for the temporal variation of solar EUV radiation between 1 and 1200 Å (Ribas et al. 2005):

$$F = 29.7 \cdot t^{-1.23} \text{ erg} \cdot \text{cm}^{-2} \cdot \text{s}^{-1}$$

where t is the stellar age in billion years. This relationship is used to convert the solar EUV energy flux in Fig. 2 to the time in Fig. 3. This relationship between the solar EUV energy flux and age of the Sun is consistent with earlier works (Zahnle and Walker 1982, Ayres 1997).

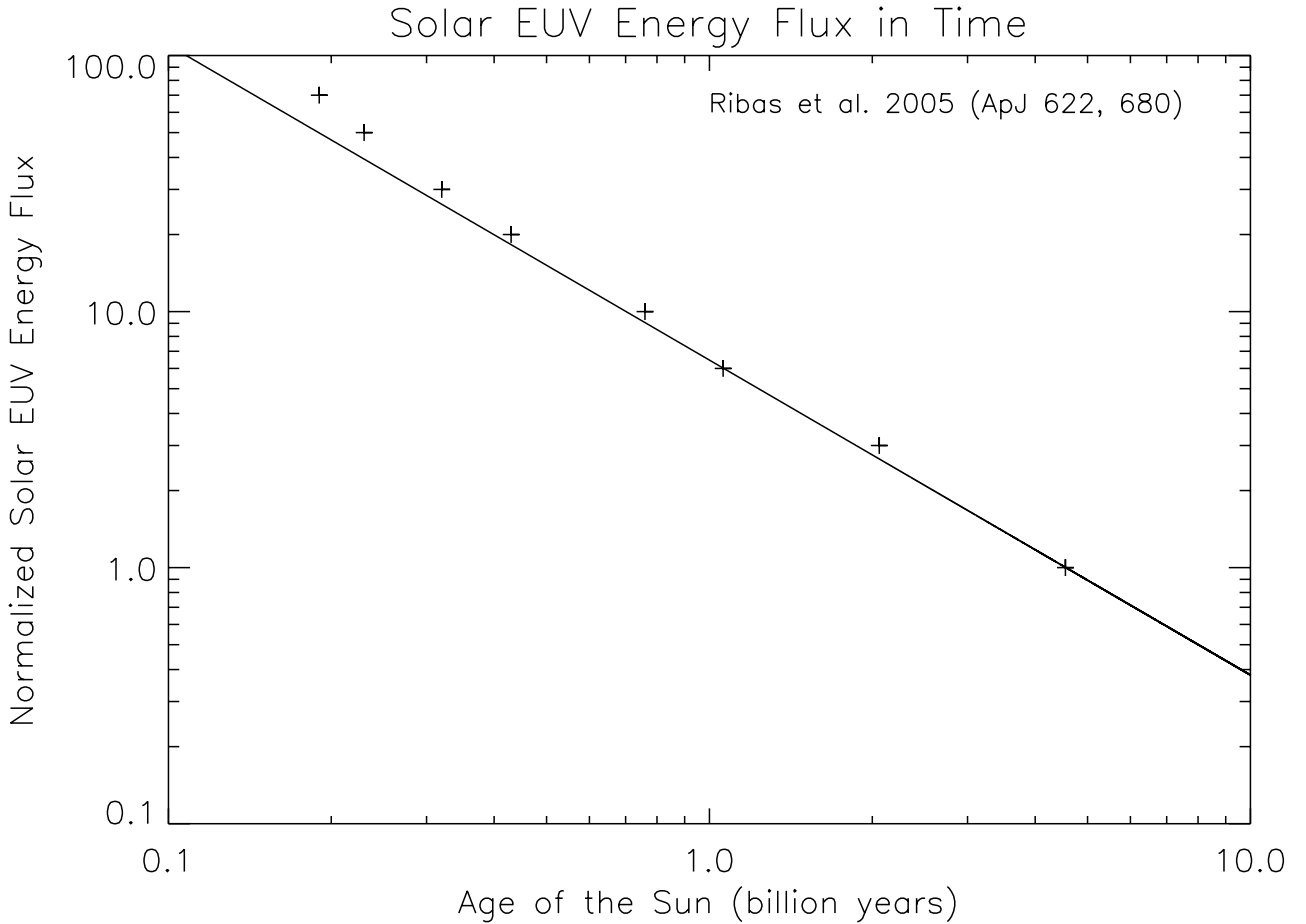


Fig. S1: variation of solar EUV energy flux with time

On the CO₂ volcanic outgassing history of early Mars:

Both Earth and Venus have about 100 bar of CO₂ today. 100-bar CO₂ on the Earth is $\sim 7 \times 10^{45}$ molecules (1-bar of CO₂ is 7×10^{43} molecules on the Earth and 3.7×10^{43} molecules on Mars). If Mars was formed from the same material as Earth, its total CO₂ reservoir could have been as much as 20 bars (7.5×10^{44} molecules). This is consistent with the estimate based on geomorphology (Carr 1986). Considering that Mars formed farther from the Sun than the Earth and thus could contain materials with volatile content 2x richer than Earth, a maximum 40-bar (1.5×10^{45} molecules) total CO₂ inventory is assumed.

It is estimated that ~1.5-bar of CO₂ was released volcanically during the late Noachian epoch during the formation of the Tharsis bulge (Phillips et al. 2001). This estimate is based on the assumption that the CO₂ content in the Tharsis magmas is the same as that of the Hawaiian basalt. If Mars magma contains more volatiles, 3-bar of CO₂ could have been released by the Tharsis system.

To obtain the lower solid line in Fig. 3, we assume that the outgassing rate decayed exponentially from 4.56 billion years ago and use the total CO₂ inventory and the Tharsis CO₂ inventory as constraints. The upper solid line in Fig. 3 is obtained by multiplying the lower line by a factor of 10.

Energy limited escape:

The energy-limited escape rate can be calculated as the following: $F_{\text{lim}} = \frac{\epsilon F_{\text{EUV}}}{4E_{\text{grav}}}$

where F_{EUV} is the solar EUV energy flux (ergs cm⁻² s⁻¹), $E_{\text{grav}} = GMm/r$ (ergs) is the potential energy of one single escaping particle, ϵ includes both the heating efficiency (the conversion factor between the absorbed solar EUV energy and the thermal energy, <1) and the altitude variation of energy absorption (>1). ϵ is set to be unity in Fig. 3. The factor of 4 accounts for the difference between the solar energy absorption area and the surface area of the planet.

References for Supplemental Materials:

- T.R. Ayres, J.G.R. 102, 1641 (1997)
M.H. Carr, Icarus 68, 187 (1986)
G. Chin, H.A. Weaver, ApJ 285, 858 (1984)
V. Dehant et al., Space Science Review 129, 279 (2007)
J.-M. Grießmeier, Aspects of the magnetosphere-stellar wind interaction of close in extrasolar planets. PhD Thesis, (2006) ISBN 3-936586-49-7, <http://dnb.ddb.de>
W.F. Huebner, J.J. Keady, S.P. Lyon, Astrophysics and Space Science 195, 1 (1992)
G. Kockarts, GRL 7, 137 (1980)
M. Lopez-Puertas, M.A. Lopez-Valverde, D.P. Edwards, F.W. Taylor, JGR 98, 8933 (1993)
I. Ribas, E.F. Guinan, M. Gudel, M. Audard, ApJ 622, 680 (2005)
U. von Zahn, S. Kumar, R. Prinn, Composition of the Venus Atmosphere, pp 299-430 in Venus, The university of Arizona press (1983)
B.E. Wood, H.-R. Müller, G.P. Zank, J.L. Linsky, ApJ 574, 412 (2002)
B.E. Wood, H.-R. Müller, G.P. Zank, J.L. Linsky, S. Redfield, ApJL 628, 143 (2005)
K.J. Zahnle, J.C.G. Walker, Rev. Geophys. 90, 6675 (1982)